CrossMark

ORIGINAL ARTICLE

A New Star-shaped Carbazole Derivative with Polyhedral Oligomeric Silsesquioxane Core: Crystal Structure and Unique Photoluminescence Property

Zixuan Xu[1] · Tianzhi Yu[1] · Yuling Zhao[2] · Hui Zhang[1] ·
Guoyun Zhao[2] · Jianfeng Li[1] · Lanqin Chai[2]

Abstract A new inorganic–organic hybrid material based on polyhedral oligomeric silsesquioxane (POSS) capped with carbazolyl substituents, octakis[3-(carbazol-9-yl)propyldimethylsiloxy]-silsesquioxane (POSS-8Cz), was successfully synthesized and characterized. The X-ray crystal structure of POSS-8Cz were described. The photophysical properties of POSS-8Cz were investigated by using UV–vis, photoluminescence spectroscopic analysis. The hybrid material exhibits blue emission in the solution and the solid film. The morphology and thermal stablity properties were measured by X-ray diffraction (XRD) and TG-DTA analysis.

Keywords Polyhedral oligomeric silsesquioxane · Carbazole derivative · Crystal structure · Photoluminescence

Introduction

Polyhedral oligomeric silsesquioxanes (POSS) unit is a cube-shaped nanoparticle in which the rigid silica-like inorganic core can be attached with eight organic functional groups at its silicon vertices [1, 2]. POSS molecules are regarded as organic–

inorganic hybrid materials at a molecular level. They are used for the development of high performance materials in medical, aerospace, microelectronics and so on [3–7]. POSS molecules can be easily synthesized to be monofunctional or multifunctional materials for commercial applications by grafting with organic functional groups. Moreover, POSS compounds may possess a high degree of compatibility in blended polymers and can easily be covalently linked into a polymer backbone [4, 8, 9]. The incorporation of POSS derivatives into polymeric materials produces nanocomposites with improved properties such as increases in glass transition temperature, thermal stability, mechanical strength, oxidation resistance and ease of processing.

The organic–inorganic hybrid materials based on POSS have attracted great interest in the last decade due to their potential applications in optical and electronic devices [3, 6, 9]. The incorporation of POSS into organic light emitting materials has led to significant improvements in the performance of organic light emitting devises (OLEDs). Since the first use of POSS as central cores for solution processed hybrid hole transport materials in OLEDs that enhanced brightness and efficiencies as compared to the devices that used traditional hole transport materials [10], the POSS functionalized light emitting materials were widely used in OLEDs. The Heeger group pioneered the use of POSS-based light emitting polymers in which POSS cores as end-cappers were attached at the chain ends of poly[2-methoxy-5-(2-ethylhexyloxy)-1,4-phenylenevinylene] (MEH-PPV) and poly(9,9-dioctylfluorene) [5]. The electroluminescent device made from the POSS-capped MEH-PPV polymer was found to exhibit higher brightness (1320 cd/m^2 at 3.5 V) and external quantum efficiency (EQE) (η_{ext}=2.2 %) than the POSS-free MEH-PPV (230 cd/m^2 at 3.5 V and η_{ext}=1.5 %). The enhanced device properties may be attributed to reduced aggregation caused by the bulky POSS end groups and improved adhesion of the polymer to the ITO coated glass substrate. Thereafter, some

research groups reported the photoluminescence and electroluminescence properties of POSS-functionalized polyfluorene materials in which POSS units were appended to the polyfluorene backbone using an alkoxy spacer [11–13]. These POSS-functionalized polyfluorene materials showed higher fluorescence quantum yields and better thermal stability than the corresponding pristine polymers because the inorganic POSS units strongly suppressed intermolecular aggregation and/or thermal oxidation and crosslinking. Additionally, the light-emitting devices fabricated with the POSS-functionalized polyfluorene materials showed much improved brightness, maximum luminescence intensity, and quantum efficiency in comparison with devices fabricated with the corresponding pristine polymers, and showed a purer blue or deep blue emission in electroluminescent devices by preventing interchain interaction and fluorenone formation. Recently, research on phosphorescent emitters and efficient light-emitting devices based on POSS materials have also attracted tremendous interest [14–16]. Very efficient white emitting OLEDs have been prepared from POSS-based blue, green, and red emitting materials. EQEs of 8.0 %, power efficiencies of 8.1 lm/W, and CIE coordinates of (0.36, 0.39) at 1000 cd/m^2 offer promise for use of solution processable POSS materials for application in white lighting.

Carbazole derivatives have high thermal stability and excellent photophysical property, they are effective hole-transporting materials and have great potential applications in many fields. Thus, the design and synthesis of new carbazole derivatives with high performance constitutes a very active area of research [17, 18]. In this work, we reported the synthesis and characterization of a new inorganic–organic hybrid material based on POSS capped with carbazolyl substituents, octakis[3-(carbazol-9-yl)propyldimethylsiloxy]-silsesquioxane (POSS-8Cz). The X-ray crystal structure, photophysical properties and thermal stablity of POSS-8Cz were investigated detailedly.

The synthetic route of POSS-8Cz was shown in Scheme 1.

Experimental

Materials and methods

Carbazole and allyl bromide were bought from Alfa Aesar. Platinum complex (platinum-1,3-divinyl-1,1,3,3-tetramethyldisiloxane, Pt-dvs, 2 wt.% Pt in xylene) were purchased from Aldrich, USA. Octakis(dimethylsiloxy)silsesquioxane ($Q_8M_8^H$) containing eight hydro-silane groups was purchased from the Hybrid Plastics Co., USA. Toluene was dried by distillation before use in the hydrosilylation reaction. All other chemicals were analytical grade reagent.

^{1}H NMR spectra were obtained on Unity Varian-500 MHz. C, H, and N analyses were obtained using an Elemental Vario-EL automatic elemental analysis instrument. UV–vis absorption and photoluminescent spectra were recorded on a Shimadzu UV-2550 spectrometer and on a Perkin-Elmer LS-55 spectrometer, respectively. Melting points were measured by using an X-4 microscopic melting point apparatus made in Beijing Taike Instrument Limited Company, and the thermometer was uncorrected.

Synthesis and characterization of octakis[3-(carbazol-9-yl)propyldimethylsiloxy]-silsesquioxane (POSS-8Cz)

9-allyl-9H-carbazole (allyl-Cz) A mixture of carbazole (10.0 g, 0.06 mol), potassium hydroxide (8.98 g, 0.16 mol) and acetone (100 mL) was stirred vigorously for 2 h at room temperature. Allyl bromide (6.6 mL, 0.072 mol) was added dropwise. After stirring for 20 h at room temperature, the reaction mixture was poured into cold water (300 mL). The mixture was extracted with CH_2Cl_2 (3×200 mL), and the combined organic phase was dried over anhydrous Na_2SO4. After filtering, the filtrate was evaporated to dryness under reduced pressure. The crude was purified by chromatography on silica gel using petroleum ether as the eluent to give allyl-

Scheme 1 The synthetic route of POSS-8Cz

Cz as a white solid (9.1 g, 73.4 %). m.p.: 51–53 °C. ^{1}H NMR (400 MHz, CDCl$_3$, δ, ppm): 8.11 (d, J=8.0 Hz, 2H), 7.46 (t, J=8.8 Hz, 2H), 7.37 (d, J=8.0 Hz, 2H), 7.25 (t, J=8.0 Hz, 2H), 6.03–5.94 (m, 1H), 5.15 (d, J=10.6 Hz, 1H), 5.05 (d, J=18.3 Hz, 1H), 4.91 (d, J=4.8 Hz, 2H). Anal. Calcd for C$_{15}$H$_{13}$N: C, 86.92; H, 6.32; N, 6.76; Found: C, 87.02; H, 6.29; N, 6.71.

POSS-8Cz Q$_8$M$_8$^{H} (200 mg, 0.196 mmol) and 9-allyl-9H-carbazole (400 mg, 1.93 mmol) were placed in a round bottom flask (100 mL). The mixture was degassed for 10 min and protected with argon, then 30 mL anhydrous toluene was added. The mixture was stirred for 15 min at room temperature, then platinum-1,3-divinyltetramethyldisiloxane (Pt-dvs) (0.02 mL) was added and the reaction mixture was stirred at room temperature for 24 h under an argon atmosphere. After the reaction was complete, the solvent was evaporated off. The crude product was purified by chromatography on silica gel using ethyl acetate/petroleum ether (1:20, v/v) as the eluent to give white solid (0.45 g, 84.7 %). m.p.: 118–120 °C. ^{1}H NMR (400 MHz, CDCl$_3$, δ, ppm): 8.06 (d, J=7.6 Hz, 16H, Ar-H), 7.39 (t, J=8.0 Hz, 16H, Ar-H), 7.28 (t, J=7.4 Hz, 16H, Ar-H), 7.18 (t, J=7.2 Hz, 16H, Ar-H), 4.10 (t, J=7.2 Hz, 16H, Cz-CH$_2$-), 1.83–1.76 (m, 16H, -CH$_2$-), 0.55 (t, J=8.4 Hz, 16H, Si-CH$_2$-), 0.02 (s, 48H, Si-CH$_3$).

Crystallography

The diffraction data were collected with a Bruker Smart Apex CCD area detector with graphite-monochromatized Mo-Kα radiation (λ=0.71073 Å) at 298(2) K. The structure was solved by using the program SHELXL and Fourier difference techniques, and refined by full-matrix least-squares method on F^2. All hydrogen atoms were added theoretically.

Results and discussion

Synthesis and characterization of POSS-8Cz

POSS-8Cz was synthesized through the hydrosilylation reaction of 9-allylcarbazole with octakis(dimethylsiloxy)silsesquioxane (Q$_8$M$_8$^{H}) in the presence of platinum(0)-1,3-divinyl-1,1,3,3-tetramethyldisiloxane (Pt-dvs) as the catalyst, as shown in Scheme 1. POSS-8Cz was soluble in common organic solvents, such as toluene, THF, chloroform, dichloromethane, and could be purified by ordinary methods. POSS-8Cz was characterized using X-ray crystallography, ^{1}H NMR, elemental analysis and X-ray diffraction (XRD) analysis.

Suitable crystal of POSS-8Cz was obtained by the evaporation of its mixtured ethyl acetate and petroleum ether solution. The crystallographic data of POSS-8Cz is shown in Table 1.
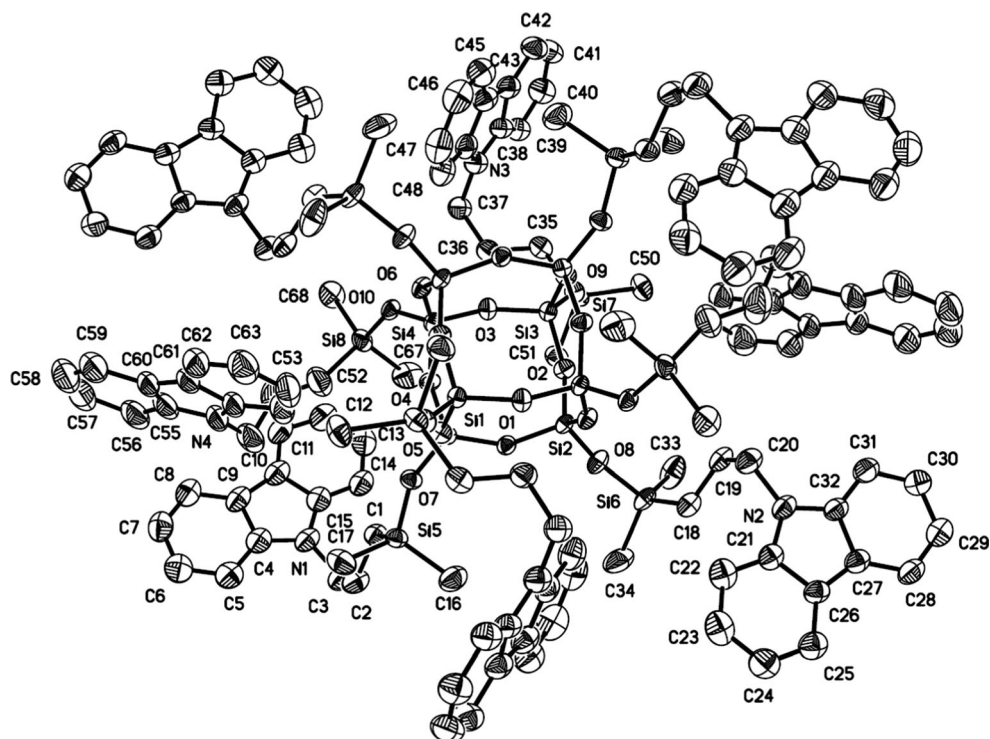
Table 1 Crystallographic and experimental data for POSS-8Cz

Empirical formula	C$_{136}$H$_{160}$N$_8$O$_{20}$Si$_{16}$
Formula weight	2676.16
Temperature (K)	298(2)
Wavelength (Å)	0.71073
Crystal system, space group	Monoclinic, C2/c
Unit cell dimensions	a=22.5956(18) Å α=90°
	b=24.7175(19) Å β=104.007(2)°
	c=27.098(2) Å γ=90°
Volume (Å^3), Z	14,684(2), 4
Calculated density (g/cm^3)	1.211
Absorption coefficient (mm^{-1})	0.202
F(000)	5672
Crystal size (mm)	0.45×0.37×0.13
θ range for data collection (°)	2.15 to 25.02
Limiting indices	−18≤h≤26, −29≤k≤29, −32≤l≤27
Reflections collected / unique	37,260/12,921 (R$_{int}$=0.0748)
Absorption correction	Semi-empirical from equivalents
Max. and min. transmission	0.9742 and 0.9144
Refinement method	Full-matrix least-squares on F^2
Data / restraints / parameters	12,921/0/819
Goodness-of-fit on F^2	1.045
Final R indices [$I>2σ(I)$]	R$_1$=0.0644, wR$_2$=0.1255
R indices (all data)	R$_1$=0.1649, wR$_2$=0.1380
Largest diff. peak and hole (eÅ^{-3})	0.585 and −0.508

The crystal structure of POSS-8Cz is given in Fig. 1. The crystal of POSS-8Cz belongs to the monoclinic space group C2/c, a=22.5956(18) Å, b=24.7175(19) Å, c=27.098(2) Å, α=γ=90°, β=104.007(2)°, U=14684(2) Å^3, Z=4, Dc=1.211 g/cm^3, μ=0.202 mm^{-1}. In this structure, the arrangement of eight carbazole groups are not identical to each other, and all eight carbazole groups do not interact with their nearest neighbors. Two carbazole groups placed on opposite Si atoms of the Si-O cage show *trans* arrangement, and two planes of carbazole groups are parallel to each other. In the eight carbazole groups, it is notable that two carbazole groups placed on opposite Si atoms (Si1 and Si1) of the Si-O cage actually fold toward the Si-O cage and the POSS core is sandwiched between the planes of two carbazole groups, and the other six carbazole groups extend away from the Si-O cage.

Figure 2 shows ^{1}H NMR spectra of POSS-8Cz, allyl-Cz, and Q$_8$M$_8$^{H}. The resonance of Si-H protons in Q$_8$M$_8$^{H} is located at 4.7 ppm (Fig. 2c). As shown in Fig. 2b, for allyl-Cz, two doublets (with fine coupling) and the quartet resonance proton resonance peaks from the allyl group in allyl-Cz are located at 5.03, 5.15 and 5.99 ppm with a relative molar ratio of 1:1:1, corresponding to iso, *trans*-
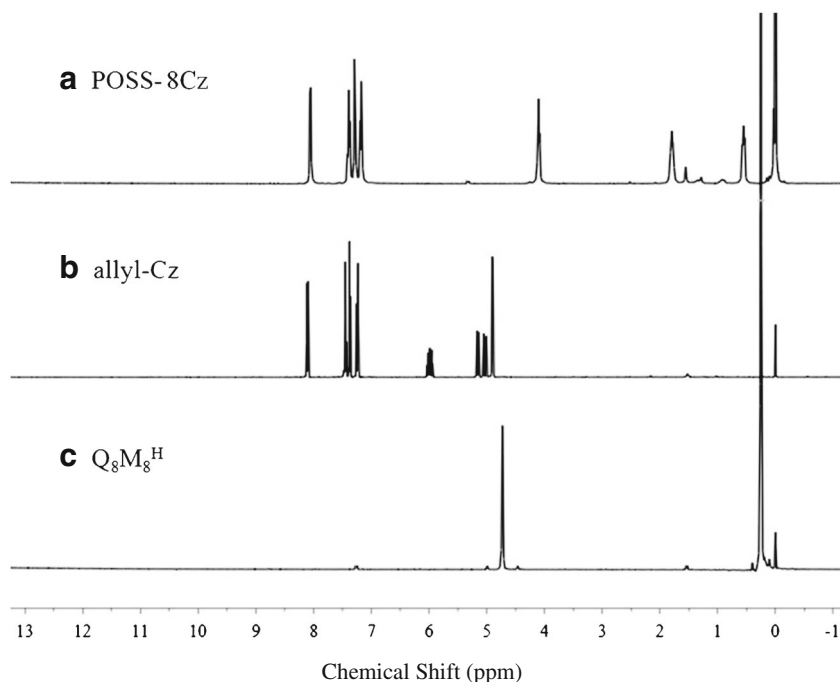
and substituted vinyl protons. The resonance of methylene (−CH$_2$-Cz) is observed at 4.90 ppm. In ^{1}H NMR spectrum of POSS-8Cz (Fig. 2a), the peaks for the vinyl group of allyl-Cz (5.03, 5.15 and 5.99 ppm) in Fig. 2b and Si-H protons (4.7 ppm) in Fig. 2c disappeared, supporting the complete hydrosilylation reaction. In addition, the resonance of methylene next to the carbazole ring is shifted from 4.90 to 4.10 ppm, and at the same time the ^{1}H

NMR spectrum of POSS-8Cz displays two resonance of methylene at 1.83 and 0.55 ppm, respectively.

Figure 3 presents the X-ray diffraction (XRD) pattern of POSS-8Cz. POSS-8Cz exhibits several sharp XRD peaks at 5.84°, 6.76°, 8.11°, 9.87°, 11.71°, 15.97° , 17.01°, 18.30° and 20.04°, and other positions also appeared lots of weak diffraction peaks, suggesting that the synthesized POSS-8Cz presents a crystal morphology.

Fig. 2 ^{1}H NMR spectra of (a) POSS-8Cz (b) Cz-allyl and (c) Q$_8$M$_8$^{H} in CDCl$_3$

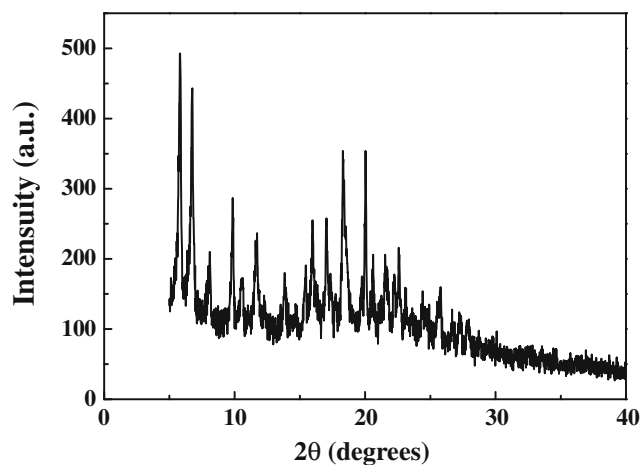Fig. 3 X-ray diffraction pattern of POSS-8Cz

Fig. 5 Normalized UV–vis absorption and photoluminescence spectra of POSS-8Cz and allyl-Cz in dichloromethane solutions. (C=1×10^{-6} mol/L)

Thermal property of POSS-8Cz

The thermogravimetry (TG) and differential thermal analysis (DTA) measurements were performed in flowing drying nitrogen atmosphere at the heating rate of 10 °C/min. The result of TG and DTA measurements of POSS-8Cz is shown in Fig. 4. From Fig. 4, it can be seen that the DTA curve shows an endothermic peak at 119 °C, but without mass loss in the TG curve, indicating that the temperature is the melting point of the compound, which is in agreement with the result obtained by a melting point apparatus. With increasing temperature, POSS-8Cz shows good thermal stability until about 450 °C. The compound begins to decompose at 453 °C, at 512 °C an endothermic peak was observed in the DTA curve, which was accompanied by a sharp weight loss in the TG curve. It shows that the compound undergoes decomposition.
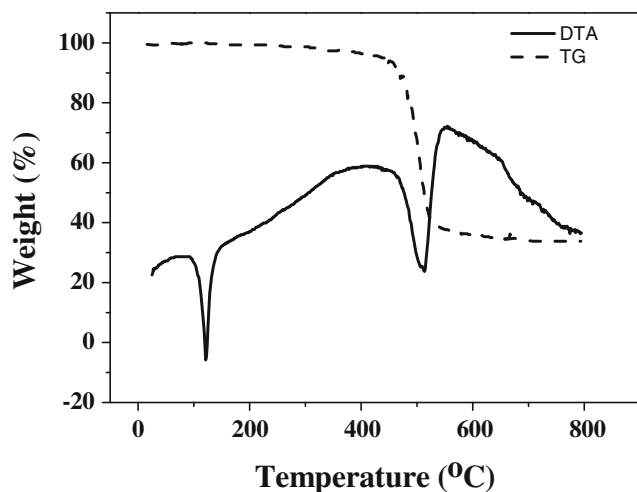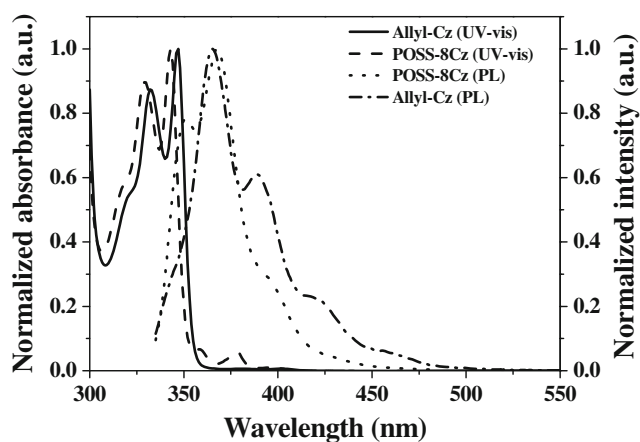
UV–vis absorption and photoluminescence spectra

The UV–vis absorption and photoluminescence spectra of POSS-8Cz and allyl-Cz were measured in diluted dichloromethane solutions, as shown in Fig. 5. Allyl-Cz exhibits two intense absorption bands at 332 and 347 nm, respectively, which can be attributed to the π-π* transitions of carbazole. The absorption shape of POSS-Cz is quite similar to that of allyl-Cz, but two intense absorption bands were blue-shifted by about 4 nm, which located at 328 and 343 nm. The photoluminescence spectrum of POSS-8Cz shows two peaks at 351 and 368 nm, while the photoluminescence spectrum of allyl-Cz presents two peaks at 365 and 389 nm. Compared with allyl-Cz, the hypsochromic shift of UV–vis absorption and photoluminescence spectra of POSS-8Cz occurs. The result indicated that each carbazole unit seems to be isolated by the rigid POSS core in the case of POSS-8Cz, so that the formation of excimer is prevented.

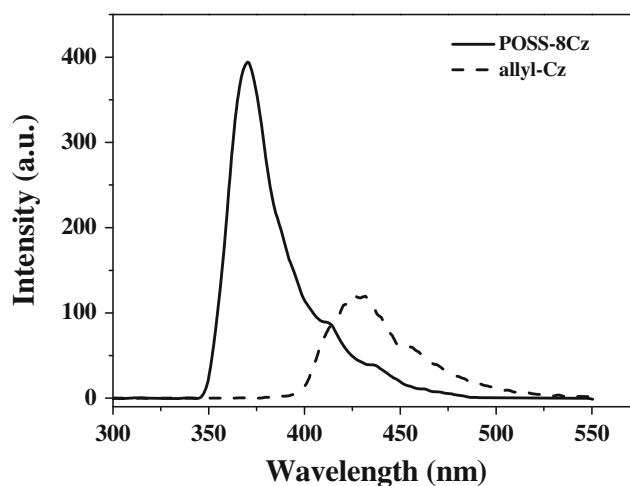Fig. 4 The therogravimetry (TG) and differential thermal analysis (DTA) of POSS-8Cz

Fig. 6 Photoluminescence spectra of POSS-8Cz and allyl-Cz in the solid state

Figure 6 illustrates photoluminescence spectra of POSS-8Cz and allyl-Cz in solid state. The photoluminescence spectrum of POSS-8Cz shows one strong emission peaks at 370 nm, while that of allyl-Cz exhibits a broad and weak emission peak at 429 nm. Due to more intermolecular interaction (π-π stacking) in the solid state, the photoluminescence spectrum of allyl-Cz is much broader than that in dichloromethane solution, and the emission peak is red-shifted to 429 nm, suggesting the formation of excimers by aggregation. For POSS-Cz, the emission shape in the solid state is different from that in dichloromethane solution, but the spectral shift is very small. It was indicated that the shape of POSS-8Cz does not strongly affect to the aggregation of carbazole moiety. This result suggests that the carbazole in POSS-8Cz is almost isolated even in the solid state, different from allyl-Cz. POSS-8Cz has eight propyl-siloxy spacers between the POSS core and carbazole groups, but the spacer length seems too short to form aggregates, and showed monomeric behavior in photoluminescence.

From the above results, it was found that the material POSS-8Cz has not only hight thermal stabily, but also should be a promising material for application in a ultraviolet OLEDs[19]. Further investigation on the ultraviolet OLEDs of POSS-8Cz is progressing at our laboratory.

Conclusions

A new inorganic–organic hybrid material of polyhedral oligomeric silsesquioxane containing carbazole, octakis[3-(carbazol-9-yl)propyldimethylsiloxy]-silsesquioxane (POSS-8Cz), was successfully synthesized by hydrosilylation reaction in the presence of platinum(0)-1,3-divinyl-1,1,3,3-tetramethyldisiloxane (Pt-dvs) as the catalyst. The structure of POSS-8Cz was characterized by single crystal X-ray crystallography and ^{1}H NMR. The compound has hight thermal stabily. The result showed that the presence of the POSS core does not affect the electronic properties because each carbazole could be effectively isolated by the steric and electronic effects.

References

1. Hartmann-Thompson C (Ed.) (2011); "Applications of Polyhedral Oligomeric Silsesquioxanes" - Advances in Silicon Science 3

2. Laine RM (2005) Nanobuilding blocks based on the [OSiO$_{1.5}$]$_x$ (x= 6, 8, 10) octasilsesquioxanes. J Mater Chem 15:3725–3744

3. Tanaka K, Chujo Y (2012) Advanced functional materials based on polyhedral oligomeric silsesquioxane (POSS). J Mater Chem 22:1733–1746

4. Phillips SH, Haddad TS, Tomczak SJ (2004) Developments in nanoscience: polyhedral oligomeric silsesquioxane (POSS)-polymers. Curr Opin Solid State Mater Sci 8:21–29

5. Xiao S, Nguyen M, Gong X, Cao Y, Wu HB, Moses D, Heeger AJ (2003) Stabilization of semiconducting polymers with silsesquioxane. Adv Funct Mater 13:25–29

6. Chan KL, Sonar P, Sellinger A (2009) Cubic silsesquioxanes for use in solution processable organic light emitting diodes (OLED). J Mater Chem 19:9103–9120

7. Pielichowski K, Njuguna J, Janowski B, Pielichowski J (2006) Polyhedral Oligomeric Silsesquioxanes (POSS)-containing nanohybrid polymers. Adv Polym Sci 201:225–296

8. Ayandele E, Sarkar B, Alexandridis P (2012) Polyhedral Oligomeric Silsesquioxane (POSS)-containing polymer nanocomposites. Nanomaterials 2:445–475

9. Wang FK, Lu XH, He CB (2011) Some recent developments of polyhedral oligomeric silsesquioxane (POSS)-based polymeric materials. J Mater Chem 21:2775–2782

10. Sellinger A, Laine RM (2003) Organic–inorganic hybrid light emitting devices (HLED), US Pat. 6517958

11. Chou CH, Hsu SL, Dinakaran K, Chiu MY, Wei KH (2005) Synthesis and characterization of luminescent polyfluorenes incorporating side-chain-tethered polyhedral oligomeric silsesquioxane units. Macromolecules 38:745–751

12. Lee J, Cho HJ, Cho NS, Hwang DH, Shim HK (2006) Synthesis of polyhedral oligomeric silsesquioxane-functionalized polyfluorenes: Hybrid organic–inorganic π-conjugated polymers. Synth Met 156:590–596

13. Lee J, Cho HJ, Cho NS, Hwang DH, Kang JM, Lim E, Lee JI, Shim HK (2006) Enhanced efficiency of polyfluorene derivatives: organic–inorganic hybrid polymer light-emitting diodes. J Polym Sci Part A: Polym Chem 44:2943–2954

14. Yang XH, Froehlich JD, Chae HS, Harding BT, Li S, Mochizuki A, Jabbour GE (2010) Efficient light-emitting devices based on platinum-complexes-anchored polyhedral oligomeric silsesquioxane materials. Chem Mater 22:4776–4782

15. Yang XH, Froehlich JD, Chae HS, Li S, Mochizuki A, Jabbour GE (2009) Efficient light-emitting devices based on phosphorescent polyhedral oligomeric silsesquioxane materials. Adv Funct Mater 19:2623–2629

16. Singh M, Chae HS, Froehlich JD, Kondou T, Li S, Mochizuki A, Jabbour GE (2009) Electroluminescence from printed stellate polyhedral oligomeric silsesquioxanes. Soft Matter 5:3002–3005

17. Brunner K, Dijken AV, Börner H, Bastiaansen JJAM, Kiggen NMM, Langeveld BMW (2004) Carbazole compounds as host materials for triplet emitters in organic light-emitting diodes: Tuning the HOMO level without influencing the triplet energy in small molecules. J Am Chem Soc 126:6035–6042

18. Zhang Q, Chen JS, Cheng YX, Wang LX, Ma DG, Jing XB, Wang FS (2004) Novel hole-transporting materials based on 1,4-bis(carbazolyl)benzene for organic light-emitting devices. J Mater Chem 14:895–900

19. Yu TZ, Su WM, Li WL, Hua RN, Chu B, Li B (2007) Ultraviolet electroluminescence from organic light emitting diode with cerium (III)-crown ether complex. Solid State Electron 51:894–899